

Physical Layer Impairments in Cascaded Multi-degree CDC ROADM斯 with NRZ and Nyquist Pulse Shaped Signals

Diogo G. Sequeira¹, Luís G. Cancela^{1,2} and João L. Rebola^{1,2}

¹*Optical Communications and Photonics Group, Instituto de Telecomunicações, Lisbon, Portugal*

²*Department of Information Science and Technology, Instituto Universitário de Lisboa (ISCTE-IUL), Lisbon, Portugal*

Keywords: ASE Noise, Broadcast and Select, In-Band Crosstalk, Nyquist Pulse, Optical Filtering, ROADM斯, Route and Select.

Abstract: Nowadays, reconfigurable optical add/drop multiplexers (ROADMs) are mainly based on broadcast and select (B&S) and route and select (R&S) architectures. Moreover, the most used components to implement the colorless, directionless and contentionless (CDC) ROADM add/drop structures are the multicast switches (MCSs) and the wavelength selective switches (WSSs). In-band crosstalk, amplified spontaneous emission (ASE) noise accumulation and optical filtering are physical layer impairments (PLIs) that become more enhanced in a CDC ROADM cascade. In this work, we investigate the impact of these PLIs in a cascade of CDC ROADM斯 based on both B&S and R&S architectures, with MCSs and WSSs-based add/drop structures and for nonreturn-to-zero (NRZ) rectangular and Nyquist pulse shaped signals. We show that the optical filtering impairment is more limiting for a R&S architecture. We also show that the ASE noise accumulation after 32 cascaded ROADM斯 leads to a 10 dB optical signal-to-noise ratio (OSNR) penalty for all ROADM degrees investigated. We have also concluded that the in-band crosstalk leads to a 1 dB OSNR penalty, after 13 and 24 cascaded 16-degree CDC ROADM斯 based on B&S for, respectively, NRZ rectangular and Nyquist pulse shapes. For a R&S architecture, the in-band crosstalk is not so harmful.

1 INTRODUCTION

The continuous and exponential increase of data traffic in recent years has been putting the optical network infrastructures in a constant pursuit of new technologies that can transport huge amounts of bits in a more cost effective and efficient way. Technologies, such as coherent detection, advanced digital signal processing, polarization division multiplexing (PDM) and wavelength division multiplexing (WDM) are now fundamental to achieve these goals (Roberts et al., 2017).

Moreover, as the data traffic becomes more heterogeneous in terms of bit rate and modulation format, and the connections duration decreases, a more dynamic, flexible and reconfigurable optical transport network is required (Jinno, 2017). These requirements can be provided by the optical network nodes, currently known as reconfigurable optical add/drop multiplexers (ROADMs) with colorless, directionless and contentionless (CDC) add/drop structures (Gringeri et al., 2010). The CDC ROADM nodes can express, add and drop any WDM signal

without restrictions and contention of wavelengths (Feuer et al., 2011).

The most used architectures to implement the ROADM nodes are the broadcast and select (B&S) and route and select (R&S) architectures (Simmons, 2014). The B&S is the cheapest implementation, but has higher insertion losses and poorer isolation than the R&S architecture. On the other hand, the R&S architecture is the best choice in terms of isolation of adjacent channels and has low insertion losses, but since it is based on wavelength selective switches (WSSs), the filtering effects are more relevant and the cost is higher than the B&S architecture.

In a multi-degree CDC ROADM-based optical network, the physical layer impairments (PLIs), such as optical filtering, amplified spontaneous emission (ASE) noise accumulation and in-band crosstalk, limit the number of ROADM nodes that an optical signal can pass along the network (Tibuleac and Filer, 2010). These PLIs are cumulative along the network and depend not only on the ROADM architecture, e.g. B&S or R&S, but also on the ROADM add/drop structures.

In the literature, some studies were performed to

address the impact of these PLIs on the network performance. In (Filer and Tibuleac, 2012), the optical filtering and in-band crosstalk impairments due to a cascade of WSSs, have been considered, but neglected the ROADM architectures types. In (Filer and Tibuleac, 2014), the impact of the ROADM architectures are considered, but the influence of the ROADM add/drop structures has been neglected. In (Pan and Tibuleac, 2016), the filtering and in-band crosstalk impact were evaluated considering the 37.5 GHz flexible grid. In that study, the authors considered a colorless add/drop structure. In (Morea et al., 2015), the impact of filtering for both the 50 GHz fixed grid and 37.5 GHz flexible grid is evaluated. In that study, the crosstalk impact is not considered, as well as the contentionless ROADM feature. In all these previous studies, the ASE noise accumulation is not considered. Instead, the authors considered that the ASE noise is totally loaded at the system input (Pan and Tibuleac, 2016) or at the system output (Morea et al., 2015).

In this work, we investigate the impact of the optical filtering, ASE noise accumulation and in-band crosstalk generated inside CDC ROADM on the network performance, through Monte-Carlo (MC) simulation. PDM quadrature phase-shift keying (PDM-QPSK) signals at 100-Gb/s, with 25 Gbaud symbol rate, for the 50 GHz fixed grid are considered, although other scenarios could be simulated (Fabregas et al., 2016). We investigate both nonreturn-to-zero (NRZ) rectangular (Wang and Lyubomirsky, 2010) and Nyquist pulse shaped signals. These last signals considered a roll-off factor (β) equal to 0.1, which is a typical value (Morea et al., 2015). This study is performed by properly modelling the ROADM nodes, considering both B&S and R&S architectures and different add/drop structures, based on multicast switches (MCSs) (Way, 2012) and WSSs (Yang et al., 2017).

This work is organized as follows. Section 2 describes the simulation model of the multi-degree CDC ROADM-based optical network. Details on the ROADM add/drop structures are provided in Subsection 2.1. In Subsection 2.2, the filtering transfer functions used to model the ROADM components are presented and characterized. The optical filtering impact is studied in Section 3, for both ROADM architectures, add/drop structures and pulse shapes signals. Section 4 investigates the in-band crosstalk level evolution in a CDC ROADM cascade also for both ROADM architectures, add/drop structures and signal shapes. In Section 5, the impact of in-band crosstalk on the network performance is evaluated. Finally, in Section 6, the

conclusions of this work are provided.

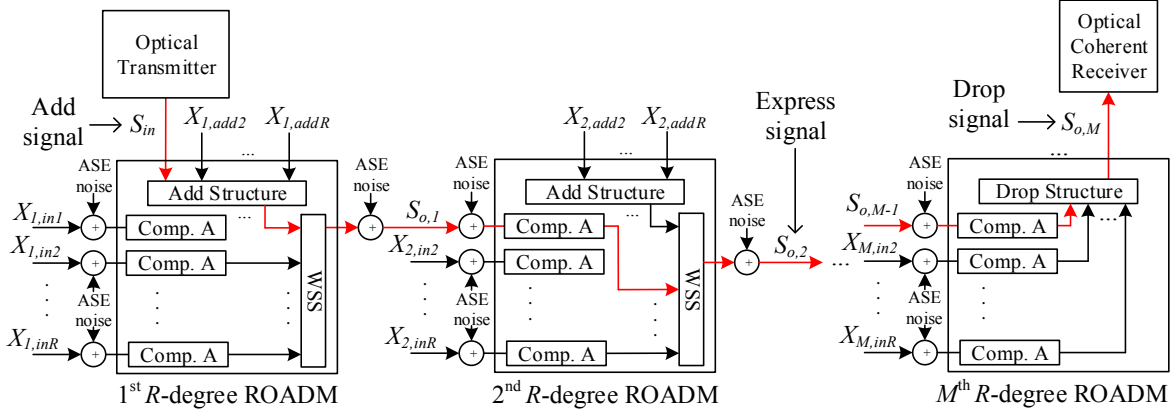
2 CDC ROADM-BASED OPTICAL NETWORK MODEL

In this section, we present the simulation model of an optical network based on multi-degree CDC ROADM, as well as, the in-band crosstalk terms generated inside these ROADM and the ASE noise added to the primary signal along the network. Subsection 2.1 describes the ROADM add/drop structures modelling. Subsection 2.2 presents the filtering transfer functions used to model the ROADM components.

Figure 1 depicts the simulation model of an optical network based on multi-degree CDC ROADM. The red line in this figure represents the light-path of the primary signal (i.e., the signal that is taken as a reference to study the impact of the PLIs), S_{in} , since it is added to the network, in the first ROADM node, until it is dropped, in the M^{th} ROADM, $S_{o,M}$. Throughout this work, we consider a 100-Gb/s NRZ rectangular or Nyquist pulse shaped signal and QPSK modulation for the primary signal. In our MC simulator, we do not consider the fiber transmission effects, so the fiber impairments are neglected.

Regarding the in-band crosstalk signals originated along the multi-degree CDC ROADM-based optical network, we consider that all interfering signals have the same modulation format and bit rate as the primary signal, but with different arbitrary transmitted symbols, characterized by a phase difference and a time misalignment between the primary signal and in-band interferers (Cancela et al., 2016). These interfering signals arise from the ROADM inputs and, also, from the ROADM add structures, denominated, respectively, $X_{M,inR}$ and $X_{M,addR}$, with M indicating the ROADM node and R the ROADM degree in which they are originated. We consider that all ROADM degrees are sources of interfering signals. In the ROADM inputs and ROADM add structures, the interfering signals pass through the respective components (e.g. WSS) and then are added to the primary signal.

Concerning the ASE noise addition, we consider that the ASE noise is added both at the ROADM inputs and outputs. The optical amplifier (OA) at the ROADM inputs is used to compensate the optical path losses, whereas the OA at the ROADM outputs is used to compensate the losses inside the ROADM node (Zami, 2013).

Figure 1: Simulation model of an optical network based on M cascaded R -degree CDC ROADM.

The node losses are considered independent of the ROADM architectures. So, in the MC simulator, we consider that all OAs have the same characteristics: noise figure, gain and optical bandwidth. Hence, they impose the same optical signal-to-noise ratio (OSNR) at its outputs. Throughout this work, the OSNRs presented correspond to the OSNR at the output of each OA and it is measured in the 0.1 nm reference bandwidth (Essiambre et al., 2010). The ASE noise is considered as an additive white Gaussian noise.

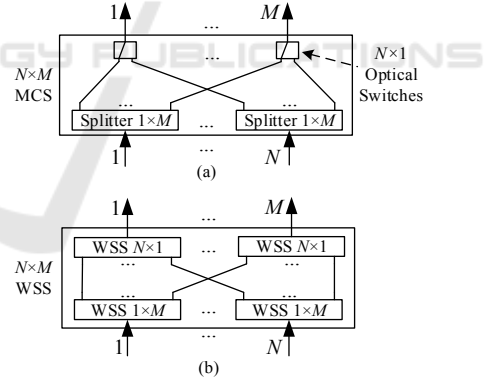
To drop the primary signal, in the last ROADM, we use an ideal coherent detection receiver model (Essiambre et al., 2010). In the decision circuit, inside the optical coherent receiver, the bit error rate (BER) is obtained by direct-error counting, for a target BER of 10^{-3} . The number of counted errors considered is 1000 and either the primary signal and the interfering signals are generated with 256 symbols. Our studies are done only for a single polarization, a 50-Gb/s QPSK signal, which corresponds to a 25 Gbaud symbol rate. We consider that polarization transmission effects are ideal and that ROADM components are polarization independent. We also assume that the optical receiver performs an ideal detection for both polarizations (Seimetz and Weinert, 2006). Hence, the results presented in this work, for a single polarization, are valid for both polarizations.

As can be observed in Figure 1, at the ROADM inputs, the signals pass through Component A, which depends on the architecture used. In ROADM nodes based on a B&S architecture, Component A is an optical splitter, while with a R&S architecture, this optical splitter is replaced by a WSS. In both architectures, at the ROADM outputs, the signals go through a WSS (Simmons, 2014). In Figure 1, to

simplify, we only show the output of one direction of the ROADM, to where the primary signal is sent.

2.1 ROADM Add/Drop Structures

In our ROADM model, we consider both MCSs and WSSs-based add/drop structures. Figure 2 depicts the model used to implement the drop structure (Colbourne and Collings, 2011). Figure 2 (a) considers a $N \times M$ MCS-based drop structure and Figure 2 (b) considers a $N \times M$ WSS-based drop structures.

Figure 2: CDC ROADM $N \times M$ drop structures based on (a) MCSs and (b) WSSs.

The corresponding model for the add structures is obtained in a similar way, by just having in mind the direction of the data flow. As can be observed from Figure 2, the MCSs are based on $1 \times M$ splitters and $N \times 1$ optical switches. As such, they are not wavelength selective as the WSS structures. In terms of in-band crosstalk generation, since inside a $N \times M$ WSS, the interfering signals pass through the isolation of two WSSs, the interferers are of second order, instead of the first order interferers that appear

on the $N \times M$ MCSs. On the other hand, the WSS structures have higher costs and are more filtering selective than the MCSs. In terms of modelling these add/drop structures, the MCSs are modelled by one filtering stage, while the WSSs are modelled by two filtering stages.

2.2 ROADMs Filtering Model

We consider two types of transfer functions to model the filtering inside the ROADM components, a transfer function for modelling the WSS pass through effect, represented by $H_p(f)$, and another transfer function for modelling the WSS blocking effect represented by $H_b(f)$. The transfer function $H_p(f)$ is modelled by a super Gaussian optical filter with lowpass equivalent transfer function given by (Pulikkaseril, 2011)

$$H_p(f) = e^{-\left[\left(\frac{f}{B_0/2}\right)^{2n} \cdot \frac{\ln 2}{2}\right]} \quad (1)$$

where n is the super Gaussian filter order, which, in this work, is set to $n = 4$, and B_0 is the -3 dB bandwidth, which is set to 41 GHz, usually used for the 50 GHz fixed grid (Filer and Tibuleac, 2012). On the other hand, the lowpass equivalent transfer function $H_b(f)$ is given by

$$H_b(f) = 1 - (1 - a) \cdot e^{-\left[\left(\frac{f}{B/2}\right)^{2n} \cdot \frac{\ln 2}{2}\right]} \quad (2)$$

where a is the blocking amplitude in linear units, $a = 10^{\frac{A[\text{dB}]}{20}}$. The -3 dB bandwidth of this stopband filter, when setting B to 41 GHz, is equal to, approximately, 48 GHz. Figure 3 shows the transfer functions, $H_p(f)$ (Figure 3 (a)) and $H_b(f)$, with $A = -40$ dB (Figure 3 (b)).

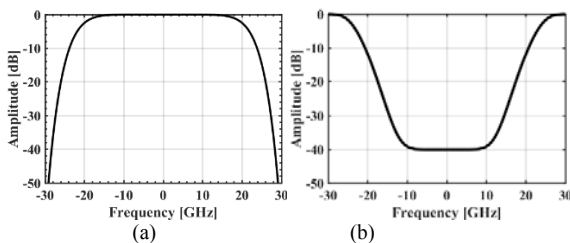


Figure 3: Transfer function of the (a) 4th order super Gaussian optical passband filter, $H_p(f)$, and (b) optical stopband filter, $H_b(f)$, with $A = -40$ dB.

3 OPTICAL FILTERING IMPACT

The impact of the optical filtering in the ROADM

cascade represented in Figure 1 is assessed in this section. The primary signal, along its light-path, passes through several filtering stages inside the ROADMs before reaching its destination. These cascaded filters lead to the narrowing of the available optical bandwidth, and, consequently, to an OSNR penalty due to the optical filtering (Hsueh, 2012). To evaluate the OSNR penalty only due to optical filtering, i.e., the difference between the required OSNR with and without the filtering impairment, we only add ASE noise at the end of the ROADM cascade, to the drop signal $S_{o,M}$ represented in Figure 1. To study the impact of the optical filtering, we neglect the in-band crosstalk interferers influence on the primary signal.

In this work, we consider a maximum of 32 ROADMs in cascade (Basch et al., 2006). Figure 4 depicts the OSNR penalty due to optical filtering as a function of the number of ROADMs based on a B&S (dashed lines) and a R&S (solid lines) architectures, for both add/drop structures: WSSs (blue lines) and MCSs (red lines) and considering NRZ rectangular signals. From Figure 4, we can conclude that, the add/drop structures do not have a significant impact in terms of OSNR penalty due to optical filtering. The difference between the OSNR penalty obtained with MCSs and WSSs-based add/drop structures is less than 0.15 dB. This difference corresponds to the additional filtering that the signal experiences when it is added and dropped with WSSs-based add/drop structures.

Regarding the difference observed, in Figure 4, between the curves for B&S and R&S architectures, the OSNR penalty due to optical filtering, as expected, is lower for a B&S architecture (Filer and Tibuleac, 2014), since with this architecture, the signal is not filtered at the ROADM inputs. For this architecture, an OSNR penalty of 1 dB is not reached after 32 cascaded ROADMs. For ROADM nodes based on a R&S architecture, penalties of ~ 1.5 dB are observed after 32 cascaded ROADMs. Considering a 1 dB OSNR penalty as the limit for this penalty, the signal can cross 20 and 22 ROADM nodes, respectively, with WSSs and MCSs-based add/drop structures.

The same studies have been done for Nyquist pulse shaped signals with $\beta = 0.1$. In this scenario, the optical filtering impact is very low, causing OSNR penalties lower than 0.1 dB after 32 cascaded ROADMs. This is explained by noting that the bandwidth of the Nyquist signals is, approximately, equal to symbol rate, 25 GHz, and the -3 dB bandwidth of the optical filters for the 50 GHz fixed grid is much larger than the symbol rate, 41 GHz,

originating a negligible OSNR penalty due to optical filtering impact, as was also reported in (Morea et al., 2015).

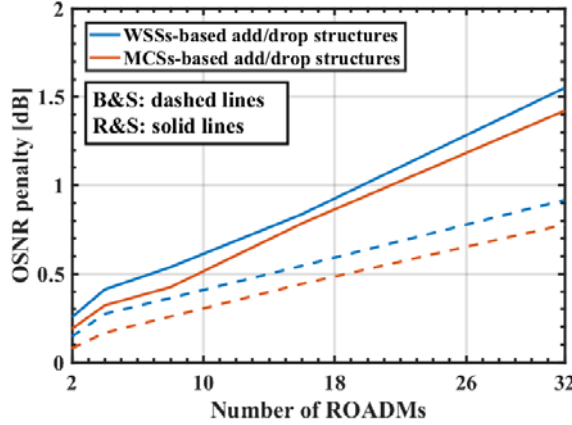


Figure 4: OSNR penalty due to optical filtering as a function of the number of ROADM, for a BER of 10^{-3} , B&S (dashed lines) and R&S (solid lines) architectures, WSSs (blue lines) and MCSs (red lines) add/drop structures and NRZ rectangular signals.

4 IN-BAND CROSSTALK LEVEL IN A CDC ROADM CASCADE

In this section, the in-band crosstalk level evolution along a cascade composed by 32 CDC ROADM is evaluated for $A = -40$ dB, several ROADM degrees, considering both ROADM architectures, different add/drop structures and rectangular and Nyquist pulse shaped signals. The crosstalk level, at each ROADM output, is defined by $X_{C,M} = P_{x,M}/P_{o,M}$, where $P_{x,M}$ is the average power of all interfering signals and $P_{o,M}$ is the primary filtered signal average power, at the output of the M^{th} ROADM (Cancela et al., 2016). The crosstalk level shown in Figures 5 and 6 is obtained by averaging the power of all crosstalk sample functions generated in the MC simulator.

Figure 5 depicts the evolution of the crosstalk level, in a cascade of 32 CDC ROADM, as a function of the number of ROADM based on a B&S (solid lines) and a R&S (dashed lines) architecture, considering NRZ rectangular signals. Figure 5 (a) considers MCSs and Figure 5 (b) considers WSSs-based add/drop structures. Several observations can be made from this figure.

First, as expected, the crosstalk level increases with the increase of the ROADM degree.

Second, for a R&S architecture, the crosstalk level along the ROADM cascade is lower than for a B&S architecture, since, the interfering signals experience more blocking filtering stages in a R&S than in a B&S architecture.

Third observation: we can see in Figure 5 (a), with MCSs-based add/drop structures, a decrease of the crosstalk level along the network for the R&S architecture (dashed lines). This can be explained by noting that the interfering signals that came from the first ROADM add structure are considered first order crosstalk terms (i.e. they pass through one stopband filter), whereas all the other interfering signals that appear along the light-path are second order terms (i.e. they pass through two stopband filters). In this way, the first order in-band terms will define the crosstalk level, which has a decrease along the ROADM cascade due to the filtering performed by the WSSs.

On the other hand, for a B&S architecture (solid lines), the interfering signals are all first order terms, so the total crosstalk level increases along the ROADM cascade, except for 2-degree ROADM. In this case, the crosstalk level decreases along the cascade until the last ROADM, where the crosstalk level increases. This behaviour occurs because in the add section of the first ROADM and in the ROADM input of the last ROADM, first order terms are originated. All the other ROADM, where the signal is expressed, do not contribute with first order terms, consequently, the ROADM filtering decreases the crosstalk level until the last ROADM. Note that, at the end of the ROADM cascade, for 16-degree ROADM with MCSs-based add/drop structures, an increase of 4 dB in the crosstalk level is observed.

Figure 5 (b) depicts the crosstalk level evolution but with WSSs-based add/drop structures. Here, we can observe a crosstalk level decreases in the last ROADM. This decrease is more abrupt for the R&S architecture, because the interfering signals pass through three stopband filters in the last ROADM node (one in the “route” WSS and two in the “drop” WSS). This crosstalk level decrease is not observed for 2-degree ROADM based on a B&S architecture (blue solid line), for the same reason mentioned in the previous paragraph. For the R&S architecture, with WSS-based add/drop structures, the crosstalk level is practically constant along the ROADM cascade, since all interfering terms generated are second order. Consequently, the crosstalk level is, mostly, defined in the first ROADM node.

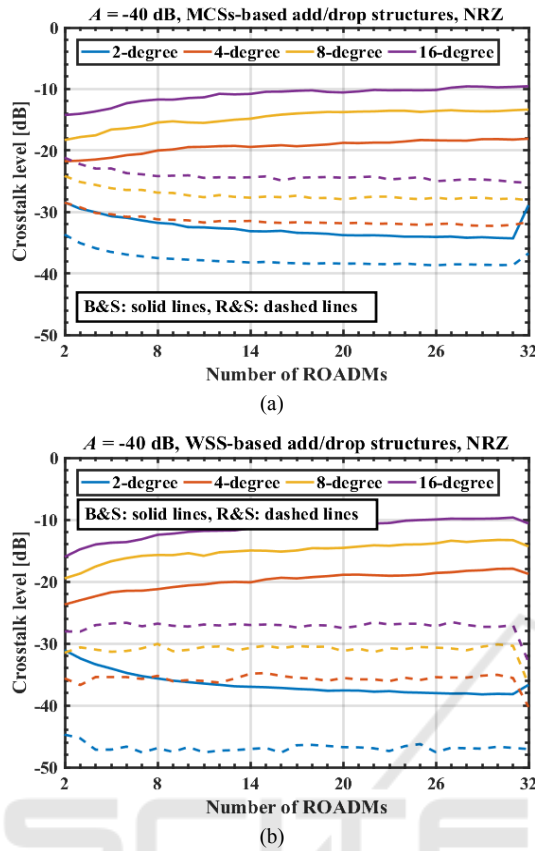


Figure 5: Crosstalk level as a function of the number of ROADM s, $A = -40$ dB, for both architectures, B&S (solid lines) and R&S (dashed lines), NRZ rectangular signals, several ROADM degrees and (a) MCSs and (b) WSSs-based add/drop structures.

Figure 6 shows the crosstalk level evolution along the ROADM cascade, but considering Nyquist pulse shaped signals. Figure 6 (a) refers to MCSs and Figure 6 (b) to WSSs-based add/drop structures.

In Figure 6 (a), for a R&S architecture (dashed lines), a constant crosstalk level along the ROADM cascade can be observed. This behaviour is justified by the fact that the interfering terms from the first ROADM add structure are first order terms, while the other interfering terms coming from the other ROADM s in the cascade, either from the ROADM inputs or from ROADM add structure, are all second order terms. Besides that, since the optical stopband filter in the first ROADM is more effective with Nyquist signals than with NRZ rectangular signals, the crosstalk level remains constant along the ROADM cascade.

For a B&S architecture (solid lines), the behavior of the crosstalk level evolution along the optical network is similar with the previously obtained for NRZ rectangular signals. Nevertheless, the crosstalk

level variation between the first and the last ROADM of the cascade, in this case, is higher than with NRZ rectangular signals. For example, for 16-degree ROADM based on a B&S architecture with MCSs-based add/drop structures, we have a variation of ~ 4 dB and ~ 11 dB, respectively, for NRZ rectangular and Nyquist pulse shaped signals. The main reason is because the stopband filters used in this work, for the 50 GHz fixed grid, provide a better blocking of in-band crosstalk interfering signals for the Nyquist pulse shaped signals, since the Nyquist signals bandwidth with $\beta = 0.1$ is, approximately, one half in comparison with the NRZ rectangular signals bandwidth. For the same reason, for Nyquist pulse shaped signals, we can observe that after two cascaded ROADM s based on a B&S architecture and with MCSs-based add/drop structures, Figure 6 (a), the crosstalk level is lower ~ 10 dB than for NRZ rectangular pulse shaped signals, Figure 5 (a).

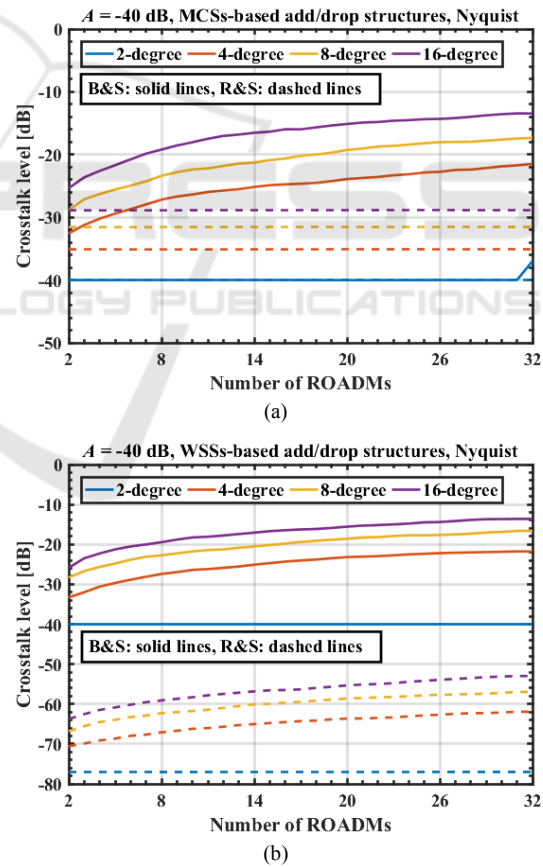


Figure 6: Crosstalk level as a function of the number of ROADM s, $A = -40$ dB, for both architectures, B&S (solid lines) and R&S (dashed lines), Nyquist pulse shaped signals, several ROADM degrees and (a) MCSs and (b) WSSs-based add/drop structures.

From Figure 6 (b), we can conclude that, with Nyquist pulse shaped signals, WSSs-based add/drop structures and a R&S architecture (dashed lines), the crosstalk levels originated are very low, below -50 dB. For a B&S architecture (solid lines), the crosstalk levels obtained are very similar with those obtained with MCSs-based add/drop structures in Figure 6 (a).

5 IN-BAND CROSSTALK IMPACT

After having studied the crosstalk level generated in a CDC ROADM cascade, for both B&S and R&S architectures, MCSs and WSSs-based add/drop structures, NRZ rectangular and Nyquist pulse shaped signals and several ROADM degrees, the OSNR penalty due to in-band crosstalk is evaluated in this section.

In the previous section, we have concluded that with $A = -40$ dB and a R&S architecture, the crosstalk levels generated along the ROADM cascade are below -20 dB. Consequently, this crosstalk level does not lead to a significant network degradation. Thus, in this section, we only study the OSNR penalty due to the in-band crosstalk for the B&S architecture.

Figure 7 shows the required OSNR, at the output of each OA, for a target BER of 10^{-3} , as a function of the number of ROADM for NRZ rectangular (solid lines) and Nyquist (dashed lines) pulse shaped signals and a B&S architecture. The same studies have been done for the R&S architecture and the required OSNRs obtained are very similar, with differences below 0.5 dB. Note that, in this work, we consider that the required OSNR is the OSNR imposed in each OA to reach a target BER of 10^{-3} at the end of the ROADM cascade. This required OSNR is measured without the in-band crosstalk impairment, but including the impact of the optical filtering and ASE noise addition in all ROADM inputs and outputs, as shown in Figure 1. In this work, we consider that all ROADM nodes introduce the same insertion losses regardless the ROADM architecture and ROADM add/drop structures. For future work, we will consider the insertion losses depending on the ROADM architectures, and, also, on the ROADM add/drop structures.

From Figure 7, we can conclude that, the required OSNR variation with the number of ROADM and the ROADM degree is very similar for both signal shapes studied. For Nyquist pulse shaped signals, there is an improvement of the

required OSNR that reaches 1 dB for 16-degree ROADM. For all ROADM degrees considered, there is a degradation of about 10 dB of the required OSNR from a cascade of 2 nodes to a cascade of 32 ROADM nodes. For example, for 2-degree ROADM, the required OSNR after 2 nodes is 19 dB and after 32 nodes, it is approximately 29 dB, for NRZ rectangular signals.

To calculate the OSNR penalty due to in-band crosstalk shown in the Figure 8 and 9, we considered the reference OSNR from the results plotted in Figure 7.

Figure 8 shows the OSNR penalty due to in-band crosstalk as a function of the number of ROADM, for a target BER of 10^{-3} , $A = -40$ dB, considering both add/drop structures, MCSs (dashed lines) and WSSs (solid lines), for several ROADM degrees and NRZ rectangular signals. From this figure, we can conclude that, for an OSNR penalty of 1 dB, the maximum number of cascaded ROADM decreases with the ROADM degree increase.

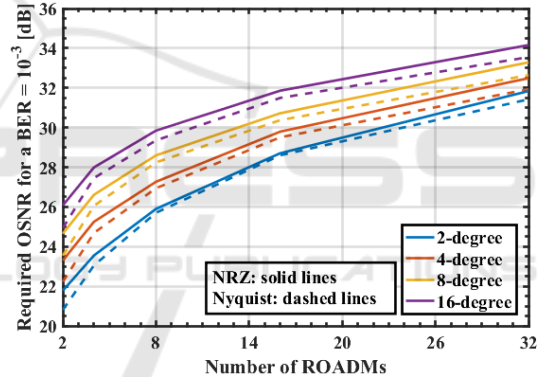


Figure 7: Required OSNR for a BER equal to 10^{-3} as a function of the number of ROADM, for the NRZ rectangular (solid lines) and Nyquist (dashed lines) pulse shaped signals, several ROADM degrees and a B&S architecture.

For example, for 8-degree ROADM, the optical signal can pass through 20 and 28 nodes, respectively, with MCSs and WSSs-based add/drop structures. While for 16-degree ROADM, where more interfering signals arise in each node, the signal can pass through 8 and 13 ROADM, respectively, with MCSs and WSSs-based add/drop structures. So, by implementing the add/drop structures with WSSs instead of MCSs, an improvement of 8 and 5 ROADM has been obtained, respectively, with degree 8 and 16.

Figure 9 shows the OSNR penalty due to in-band crosstalk as a function of the number of 16-degree ROADM, for NRZ rectangular (red lines) and

Nyquist (blue lines) pulse shaped signals. From this figure, we can observe a significant improvement on the ROADM number that an optical signal can pass with the Nyquist pulse shape. An OSNR penalty of 1 dB is reached after 13 and 24 cascaded 16-degree ROADM, for, respectively, NRZ rectangular and Nyquist pulse shaped signals and with WSSs-based add/drop structures. It means an improvement of 11 ROADM. For MCSs-based add/drop structures, the improvement is about 15 ROADM. This improvement is related with the crosstalk level at the end of the ROADM cascade, which is higher for NRZ rectangular signals than for Nyquist pulse shaped signals, as shown in Figures 5 and 6.

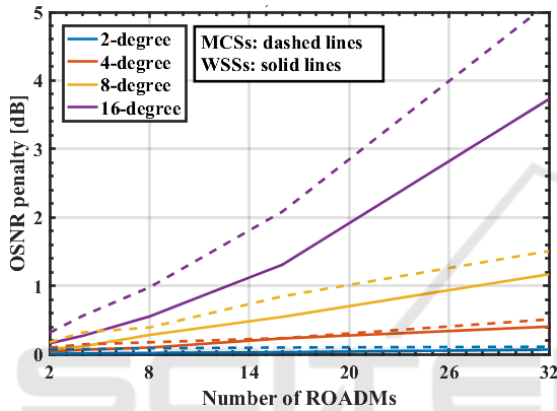


Figure 8: OSNR penalty due to the in-band crosstalk as a function of the number of ROADM nodes, for a BER of 10^{-3} , $A = -40$ dB, add/drop structures based on MCSs (dashed lines) and on WSSs (solid lines) and NRZ rectangular signals.

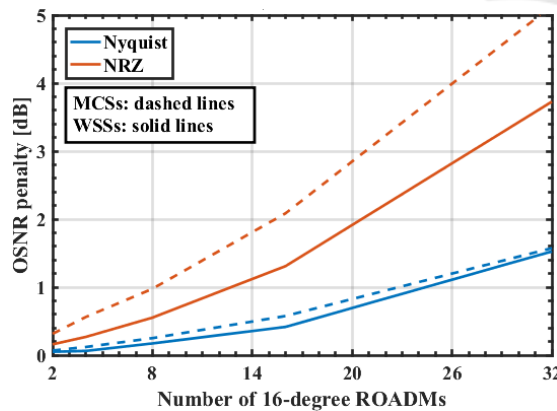


Figure 9: OSNR penalty due to in-band crosstalk as a function of the number of 16-degree ROADM nodes, for a BER of 10^{-3} , $A = -40$ dB, add/drop structures based on MCSs (dashed lines) and on WSSs (solid lines) and for NRZ rectangular (red lines) and Nyquist (blue lines) pulse shaped signals.

Comparing the impact of the ASE noise accumulation with the in-band crosstalk impact in a CDC ROADM cascade, we can conclude that, the ASE noise accumulation has a greater impact than the in-band crosstalk in terms of OSNR penalty. As referred, at the end of a cascade with 32 ROADM, the ASE noise accumulation leads to an OSNR penalty of, approximately, 10 dB. The in-band crosstalk, in the worst case (i.e., with NRZ rectangular signals, MCSs-based add/drop structures, a B&S architecture and 16-degree ROADM) leads to an OSNR penalty slightly higher than 5 dB.

6 CONCLUSIONS

In this work, we have investigated the impact of PLIs, namely, optical filtering, in-band crosstalk and ASE noise accumulation in a CDC ROADM cascade for both B&S and R&S architectures and with MCSs and WSSs-based add/drop structures. Our studies have been performed considering 100-Gb/s QPSK signals for the 50 GHz fixed grid with NRZ rectangular and Nyquist pulse shapes.

Our results showed that the impact of the optical filtering with NRZ rectangular signals and a R&S architecture is more significant than with a B&S architecture. For CDC ROADM based on a R&S architecture, the optical signal can pass through 20 and 22 ROADM nodes, respectively, with WSSs and MCSs-based add/drop structures, until an OSNR penalty of 1 dB is reached. The B&S architecture does not lead to an OSNR penalty of 1 dB at the end of 32 cascaded ROADM. For Nyquist shaped signals, we have observed that the impact of optical filtering is negligible, for both ROADM architectures.

In terms of the in-band crosstalk level generated in a ROADM cascade, we have concluded that, for a R&S architecture, the crosstalk level is below -20 dB due to the enhanced signal blocking imposed by the higher number of WSSs in the light-path. In ROADM based on a B&S architecture, the OSNR penalty due to in-band crosstalk is higher with MCSs-based add/drop structures. An OSNR penalty of 1 dB is reached after a NRZ rectangular QPSK signal passes through 20 and 8 CDC ROADM nodes, respectively, with degree 8 and 16. An improvement is reached using WSSs-based add/drop structures. The OSNR penalty of 1 dB due to in-band crosstalk is reached at the end of 28 and 13 cascaded ROADM, respectively, with degree 8 and 16. For Nyquist pulse shaped signals, the OSNR

penalty is lower than for NRZ rectangular signals, for both add/drop structures. Our results showed an improvement of 15 and 11 ROADM斯 in cascade with Nyquist pulse shapes for 16-degree ROADM斯, and, respectively, MCS and WSSs-based add/drop structures.

We, also, have seen that, the ASE noise accumulation along the ROADM cascade leads to a 10 dB OSNR degradation after 32 cascaded ROADM斯 and should be considered as a limitation factor to the number of ROADM斯 that a signal can cross in an optical network.

ACKNOWLEDGEMENTS

This work was supported by Fundação para a Ciência e Tecnologia (FCT) of Portugal within the project UID/EEA/50008/2013.

REFERENCES

- Basch, E., et al. (2006). Architectural tradeoffs for reconfigurable dense wavelength-division multiplexing systems. *IEEE J. Sel. Top. Quantum Electron.*, 12(4), 615-626.
- Cancela, L., et al. (2016). Analytical tools for evaluating the impact of in-band crosstalk in DP-QPSK signals. *NOC*, 6-11.
- Colbourne, P. and Collings, B. (2011). ROADM Switching Technologies. *OFC*, pp. OTuD1.
- Essiambre, R., (2010). Capacity limits of optical fiber networks. *J. Lightw. Technol.*, 28(4), 662-701.
- Fabrega, J., et al. (2016). On the filter narrowing issues in elastic optical networks. *J. Opt. Commun. Netw.*, 8(7), A23-A33.
- Feuer, M., et al. (2011). Intra-node contention in dynamic photonic networks. *J. Lightw. Technol.*, 29(4), 529-535.
- Filer, M. and Tibuleac, S. (2012). Generalized weighted crosstalk for DWDM systems with cascaded wavelength-selective switches. *Opt. Exp.*, 20(16), 17620-17631.
- Filer, M. and Tibuleac, S. (2014). N-degree ROADM architecture comparison: Broadcast-and-select versus route-and-select in 120 Gb/s DP-QPSK transmission systems. *OFC*, pp. Th1I-2.
- Gringeri, S., et al. (2010). Flexible architectures for optical transport nodes and networks. *IEEE Commun. Mag.*, 48(7), 40-50.
- Hsueh, Y., et al. (2012). Passband narrowing and crosstalk impairments in ROADM-enabled 100G DWDM networks. *J. Lightw. Technol.*, 30(24), 3980-3986.
- Jinno, M. (2017). Elastic optical networking: Roles and benefits in beyond 100-Gb/s era. *J. Lightw. Technol.*, 35(5), 1116-1124.
- Morea, A., et al. (2015). Throughput comparison between 50-GHz and 37.5-GHz grid transparent networks. *J. Opt. Commun. Netw.*, 7(2), A293-A300.
- Pan, J. and Tibuleac, S. (2016). Filtering and crosstalk penalties for PDM-8QAM/16QAM super-channels in DWDM networks using broadcast-and-select and route-and-select ROADM斯. *OFC*, pp. W2A-49.
- Pulikkaseril, C. (2011). Spectral modeling of channel band shapes in wavelength selective switches. *Opt. Exp.*, 19(9), 8458-8470.
- Roberts, K., et al. (2017). Beyond 100 Gb/s: capacity, flexibility, and network optimization. *J. Opt. Commun. Netw.*, 9(4), C12-C24.
- Seimetz, M. and Weinert, C. (2006). Options, feasibility, and availability of 2×4 90° hybrids for coherent optical systems. *J. Lightw. Technol.*, 24(3), 1317-1322.
- Simmons, J. (2014). *Optical network design and planning*. Springer, 2nd edition.
- Tibuleac, S. and Filer, M. (2010). Transmission impairments in DWDM networks with reconfigurable optical add-drop multiplexers. *J. Lightw. Technol.*, 28(4), 557-598.
- Wang, Y. and Lyubomirsky, I. (2010). Impact of DP-QPSK pulse shape in nonlinear 100 G transmission. *J. Lightw. Technol.*, 28(18), 2750-2756.
- Way, W. (2012). Optimum architecture for M×N multicast switch-based colorless, directionless, contentionless, and flexible-grid ROADM. *OFC*, pp. NW3F-5.
- Woodward, S., et al., (2010). Intra-node contention in a dynamic, colorless, non-directional ROADM. *OFC*.
- Yang, H., et al. (2017). Low-cost CDC ROADM architecture based on stacked wavelength selective switches. *J. Opt. Commun. Netw.*, 9(5), 375-384.
- Zami, T. (2013). Current and Future Flexible Wavelength Routing Cross-Connects. *Bell Labs Technical Journal*, 18(3), 23-38.